Adsorptive removal of cochineal red a dye from aqueous solutions using yeast

Martyna Borysiak, Elżbieta Gabruś*

West Pomeranian University of Technology, Szczecin, Faculty of Chemical Technology
and Engineering, Piastów 42, 71-065 Szczecin, Poland

This paper presents an experimental study on Cochineal Red A dye adsorptive removal by yeast. Batch equilibrium and kinetic tests were conducted in constant temperature of 30 °C for the dye's initial concentration range of 0.02–0.50 g/L (pH = 3 and 10) and 0.02–0.35 g/L (pH = 7.6). The equilibrium was reached after 105–120 min. Yeast demonstrated the adsorption capacity of 10.16 mg/g for acidic environment (pH = 3) and slightly lower values (8.13 mg/g and 8.38 mg/g respectively) for neutral (pH = 7.6) and alkaline environment (pH = 10). The experimental equilibrium results were fitted with Langmuir, Freundlich, Sips and Toth isotherm models. Most of them (Freundlich model being the exception) were proven sufficient for the experimental data correlation. The adsorption kinetic studies showed that the pseudo-second order model fits better the experimental data than the pseudo-first-order model. Results achieved from intra-particle diffusion model indicate that powdered yeast are a nonporous adsorbent. The percentage of solution discoloration reached a maximum value of 75% at pH = 3 for an initial dye concentration of 0.02 g/L.

Keywords: adsorption of dyes, isotherms, kinetics, yeast

1. INTRODUCTION

Nowadays, water contamination, which is associated with the increase in human population, is one of the growing problems of the world (Basile et al., 2015; Wang et al., 2010). One of the common pollutants are synthetic dyes released to the environment with industrial wastewaters (Basile et al., 2015; Tan et al., 2007). Based on their chemical structure, dyes are classified into multiple groups. The largest group of synthetic dyes is called azo dyes (Gupta and Suhas, 2009). Some of those are proven to be toxic, especially in long term contact with living organisms. Potentially mutagenic and carcinogenic properties are followed by intense coloration of water visible for naked eye even at very low concentrations of dyes (Rafatullah et al., 2010; Rida et al., 2013; Tan et al., 2007). For these reasons, it is very desirable to remove the dyes from wastewaters. As a representative of azo dye group, Cochineal Red A was selected for experiments. Liquid phase adsorption was proven to be an effective method of dye removal from wastewaters. Among adsorbents, commercial active carbon shows very high adsorption capacity, but due to the resources it is obtained from, it is considered rather costly (El-Sayed, 2011; Kavitha and Namasivayam, 2007). This leads to continuous attempts to find relatively low-cost, non-commercial adsorbents that could be used in the process. Among materials such as saw dusts obtained from different kinds of trees, fruit peels, shells and clays, also the use of yeast was noted (Gupta and Suhas, 2009; Rafatullah et al., 2010; Yagub et al., 2014).

---

* Corresponding author, e-mail: Elzbieta.Gabrus@zut.edu.pl

www.czasopisma.pan.pl   PAN   www.journals.pan.pl

M. Borysiak, E. Gabruś, Chem. Process Eng., 2020, 41 (2), 105–117

The aims of this work are (i) evaluation of adsorption affinity of yeast towards Cochineal Red A dye; (ii) finding the best fitting isotherm model based on different quality assessment methods; (iii) identification of dye adsorption on powdered yeast process mechanism based on kinetic models.

2. MATERIALS AND METHODS

2.1. Adsorbent and dye solutions

In the experiments, powdered yeast (*Saccharomyces cereviasiae*) purchased from Sigma-Aldrich was used. The concentration of the adsorbent was in the range of 15.0-16.0 g/L. The dye used to prepare the solutions for adsorption was commercially available Cochineal Red A (CAS Number: 51811-48-4, chemical formula: $C_{20}H_{11}N_2Na_3O_{10}S_3$, molar mass 561.5 g/mol) The initial dye concentration for pH = 3 and pH = 10 varied in the range of 0.02-0.50 g/L, while for pH = 7.6 in the range of 0.02-0.35 g/L. Environment modifications were achieved by addition of hydrochloric acid (pH = 3) or sodium hydroxide (pH = 10), both manufactured by CHEMPUR.

2.2. Adsorption procedure

The dye solutions with known concentrations (200 mL each) were put in conical flasks with glass corks and settled in water bath shaker with temperature control ELPIN+ water bath shaker type 357 (ELPIN+, Poland). The temperature was set to 30 °C. When the temperature of the solutions reached the set value, pre-prepared amounts of powdered yeast (about 3 g per 200 mL of the dye solution) were put in the solutions and formed suspensions. Samples for dye concentration analysis were taken in set intervals of time. For the separation of clear liquid from the suspension, EBA 200 centrifuge (Hettich, Germany) was used. Afterwards, the absorbance of the samples was measured with a UV-MINI 1240 (Shimadzu, Japan) at wavelength values 511 nm (pH = 7.6) and 507 nm (pH = 3 and pH = 10). Dye concentrations were calculated from calibration curves – linear correlations between dye concentration in the solution and the solution's absorbance. When the adsorption equilibrium was reached, the experiment was ended (105 minutes for pH = 3 and pH = 10, 120 minutes for pH = 7.6).

3. RESULTS AND DISCUSSION

3.1. Equilibrium studies

The results achieved were processed to acquire the values of equilibrium adsorption, and based on that, equilibrium adsorption isotherms.

The first step was calculating equilibrium adsorption from the mass balance equation for every test run (Eq. (1)).

$$q_e = \frac{(C_0 - C_e) \cdot V}{m_{ads}} \qquad (1)$$

The experimental data points were described with selected isotherm models using STATISTICA software.

3.2. Langmuir isotherm model

Langmuir isotherm model is a two-parameter empirical equation that assumes monolayer formation on the adsorbent's surface, which has a finite amount of adsorption sites with the same adsorbent affinity (Foo and Hameed, 2010; Worch, 2012). Langmuir model is represented by Eq. (2).

$$q_e = \frac{q_L b C_e}{1 + b C_e} \tag{2}$$

3.3. Freundlich isotherm model

Used often for equilibrium characteristics in water treatment processes, Freundlich model (Eq. (3)) is not limited to monolayer adsorption. Providing inadequate fit for very low and very high concentrations, it can represent the middle range quite well (Howe et al., 2012; Worch, 2012; Yagub et al., 2014).

$$q_e = K_F C_e^{\frac{1}{n}} \tag{3}$$

3.4. Sips isotherm model

Also called the Langmuir-Freundlich model, Sips isotherm equation (Eq. (4)) combines both previously mentioned models (Bonilla-Petriciolet et al., 2017; Foo and Hameed, 2010).

$$q_e = \frac{K_S a_S C_e^{\beta}}{1 + a_S C_e^{\beta}} \tag{4}$$

3.5. Toth isotherm model

The Toth isotherm model (Eq. (5)) is an empirical equation proven to be effective for heterogeneous adsorption systems. It is based on the assumption that most of the sites' sorption energy is smaller than its mean value (Foo and Hameed, 2010; Ho et al., 2002; Vijayaraghavan et al., 2006).

$$q_e = \frac{K_T C_e}{(a_T + C_e)^{\frac{1}{T}}} \tag{5}$$

Experimental adsorption isotherms and fitted models for different pH values were presented in Fig. 1. The values of calculated isotherm model coefficients were shown in Table 1.

3.6. Quality of fit evaluation

Several error measurements were used to evaluate the quality of fit of four above mentioned adsorption isotherm models. Those methods were: coefficient of determination, average relative error, sum-of squares of errors, Chi-squared statistics, root mean sum-of-squares error and normalized standard deviation (Tan and Hameed, 2017). The value of determination coefficient varies between 0 and 1, where 1 means ideal linear relationship (Montgomery et al., 2012). For all of the remaining measurements, the smaller the calculated value, the better fitting is provided by the model. The calculated values of all error measurements were presented in Table 1.

www.czasopisma.pan.pl   PAN   www.journals.pan.pl

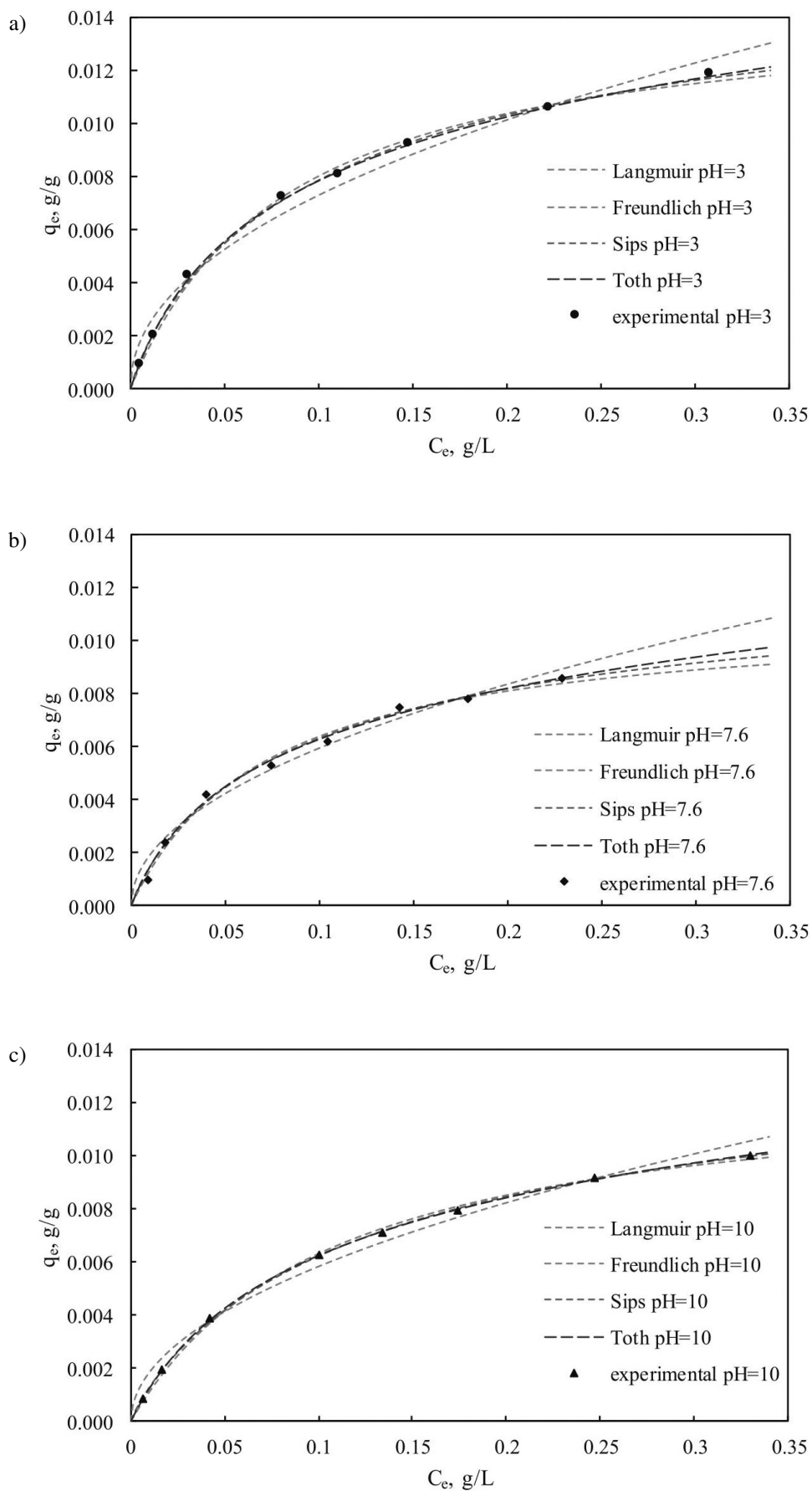*M. Borysiak, E. Gabruś, Chem. Process Eng., 2020, 41 (2), 105–117*

Fig. 1. Experimental data points and isotherm models (Langmuir, Freundlich, Sips and Toth) achieved
for a) pH = 3; b) pH = 7.6; c) pH = 10

Table 1. Isotherm models constants calculated from experimental data and error measurements

	pH = 3	pH = 7.6	pH = 10
Langmuir isotherm			
q_L, g/g	0.01469	0.01110	0.01308
b, L/g	11.98106	13.63495	9.32847
R^2, –	0.997	0.992	0.998
δ, %	3.72	5.83	3.54
SSE, –	3.30E-07	3.96E-07	1.26E-07
χ^2, –	5.94E-05	1.03E-04	3.67E-05
RMSE, –	2.03E-04	2.23E-04	1.25E-04
Δq, %	0.26	0.60	0.25
Freundlich isotherm			
K_F, (L^{1n}/g^{1n})	0.0217	0.0185	0.0183
n, –	2.1093	2.0336	2.0085
R^2, –	0.979	0.978	0.983
δ, %	19.65	13.67	15.97
SSE, –	2.40E-06	1.11E-06	1.36E-06
χ^2, –	7.41E-04	4.32E-04	4.79E-04
RMSE, –	5.47E-04	3.73E-04	4.13E-04
Δq, %	14.68	8.92	10.37
Sips isotherm			
K_S, L/g	0.0166	0.0127	0.0148
β, –	0.8713	0.8757	0.8803
a_S, $(L/g)^{\beta}$	6.7057	7.4637	5.4946
R^2, –	0.999	0.994	1.000
δ, %	3.89	6.78	1.96
SSE, –	1.60E-07	3.29E-07	2.91E-08
χ^2, –	4.24E-05	1.20E-04	1.20E-05
RMSE, –	1.42E-04	2.03E-04	6.03E-05
Δq, %	0.35	1.43	0.17
Toth isotherm			
K_T, L/g	0.0167	0.0135	0.0143
a_T, $(g/L)^{1/T}$	0.0395	0.0333	0.0538
T, –	1.2710	1.3146	1.2728
R^2, –	0.999	0.995	1.000
δ, %	2.50	6.06	0.75
SSE, –	7.79E-08	2.74E-07	1.40E-08
χ^2, –	1.99E-05	9.99E-05	2.32E-06
RMSE, –	9.87E-05	1.85E-04	4.19E-05
Δq, %	0.13	1.23	0.02

www.czasopisma.pan.pl   PAN   www.journals.pan.pl

M. Borysiak, E. Gabruś, Chem. Process Eng., 2020, 41 (2), 105–117

Coefficient of determination (R^2, –)

$$R^2 = 1 - \frac{\sum_{i=1}^{n} \left(q_{calc} - \bar{q}_{exp}\right)^2}{\sum_{i=1}^{n} \left(q_{exp} - \bar{q}_{exp}\right)^2} \tag{6}$$

Average relative error (δ, %)

$$\delta = \frac{1}{n} \sum_{i=1}^{n} \left| \frac{q_{exp} - q_{cal}}{q_{exp}} \right| \tag{7}$$

Sum-of-squares of errors (SSE, –)

$$SSE = \sum_{i=1}^{n} \left(q_{cal} - q_{exp}\right)^2 \tag{8}$$

Chi-squared statistics (χ^2, –)

$$\chi^2 = \sum_{i=1}^{n} \frac{\left(q_{exp} - q_{cal}\right)^2}{q_{cal}} \tag{9}$$

Root mean sum-of-squares error (RMSE, –)

$$RMSE = \sqrt{\frac{1}{n} \sum_{i=1}^{n} \left(q_{exp} - q_{cal}\right)^2} \tag{10}$$

Normalized standard deviation (Δq, %)

$$\Delta q = 100 \sqrt{\frac{1}{n-1} \sum_{i=1}^{n} \left(\frac{q_{exp} - q_{cal}}{q_{exp}}\right)^2} \tag{11}$$

For Langmuir, Sips and Toth isotherm models the values of determination coefficient R^2 are 0.992 and higher, which indicates a very good fit of the models to the experimental data. Average relative error δ has the largest value that amounts to 6.78% (Sips isotherm model, pH = 7.6) and the smallest value 0.75% (Toth isotherm model, pH = 10). The values of sum-of-squares of errors SSE, Chi-squared statistics χ^2 and root mean sum-of-squares error $RMSE$ are the lowest for Toth isotherm model for all of pH values. Normalized standard deviation reached the smallest value of 0.02% (Toth isotherm model, pH = 10) and the highest value that amounted to 1.43% (Sips isotherm model, pH = 7.6).

Freundlich model deviates far from the experimental results. The values of the coefficient of determination R^2 vary from 0.978 to 0.983. Average relative error δ is in range from 13.67% to 19.65%. The values of the remaining error measurements are all higher than for other isotherm models.

Maximum adsorption capacity that amounted to 10.16 mg/g was achieved in acidic environment. Another research of Cochineal Red A (Acid Red 18) adsorption demonstrated 10.84 mg/g of maximum adsorption capacity for activated carbon prepared from walnut wood and 10.4 mg/g of maximum adsorption capacity for activated carbon prepared from poplar wood (Heibati et al., 2015). In case of activated carbon prepared from walnut and poplar woods, both system adsorption results fitted well with Freundlich model (Heibati et al., 2015). Another study of poplar wood activated carbon has shown that Langmuir model also provided good quality of fit for the experimental data (Shokoohi et al., 2010).

3.7. Adsorption kinetic studies

The Cochineal Red A dye adsorption kinetics is fast and the equilibrium is reached within two hours. The kinetic curves were evaluated using pseudo-first order (Eq. (12)), pseudo-second order (Eq. (13)) and intra-particle diffusion (Eq. (14)) models.

3.7.1. Pseudo-first order kinetic model

Pseudo-first order kinetic model, developed by Lagergren, is often used to characterize liquid phase adsorption (Heibati et al., 2015; Tan and Hameed, 2017; Yuh-Shan H, 2004; Wang et al., 2010) as it is based on solid adsorption capacity (Bonilla-Petriciolet et al., 2017; Ho and McKay, 1999; Yuh-Shan, 2004). It was reported that this model may not be valid for systems, where adsorption time exceeds 20-30 minutes (Aksu, 2005; Bonilla-Petriciolet et al., 2017; Gerente et al., 2007; Tan and Hameed, 2017). This model usually fits an assumption that for higher initial concentrations, longer time is needed to reach the equilibrium (Plazinski et al., 2009; Tan and Hameed, 2017). The linear form of the equation is presented below.

$$\ln\left(\frac{q_e}{q_e - q_t}\right) = k_1 t \tag{12}$$

Pseudo-first order kinetic model resulted in an inadequate fit to the experimental data. The results achieved for different pH and the same initial concentrations were shown in Fig. 2 as a plot of $\ln(q_e - q_t)$ vs t.
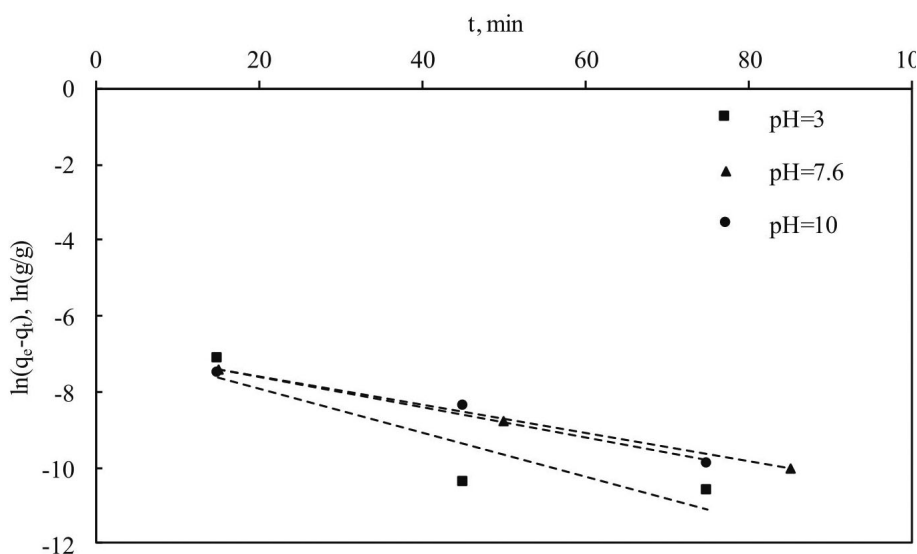

Fig. 2. Linear pseudo-first order kinetic model for initial dye concentration $C_0 = 0.25$ g/L

3.7.2. Pseudo-second order kinetic model

Pseudo-second order kinetic model follows the assumption that the overall sorption kinetics is controlled by the rate of direct sorption process (Plazinski et al., 2009). Reports were made that it often provides a very high correlation to the experimental results (Frantz et al., 2017; Ho and McKay, 1999; Plazinski et al., 2009; Rehman et al., 2018). The linear form of pseudo-second order kinetic model was shown as Eq. (13).

$$\frac{t}{q_t} = \frac{1}{k_2 q_e^2} + \frac{t}{q_e} \tag{13}$$

The calculated values of pseudo-second order kinetic model rate constant k_2 for different initial concentrations of dye and pH values were presented in Table 2.

For diluted dye solutions the adsorption rate is visibly faster than for more concentrated ones (higher k_2 values). The achieved coefficient of determination value varied from 0.998 to 1, which indicates a very strong linear relationship thus good quality of fit.

Linearization of pseudo-second order kinetic model in a graphic form as a plot of t/q_t vs t was presented in Fig. 3.

www.czasopisma.pan.pl   PAN   www.journals.pan.pl

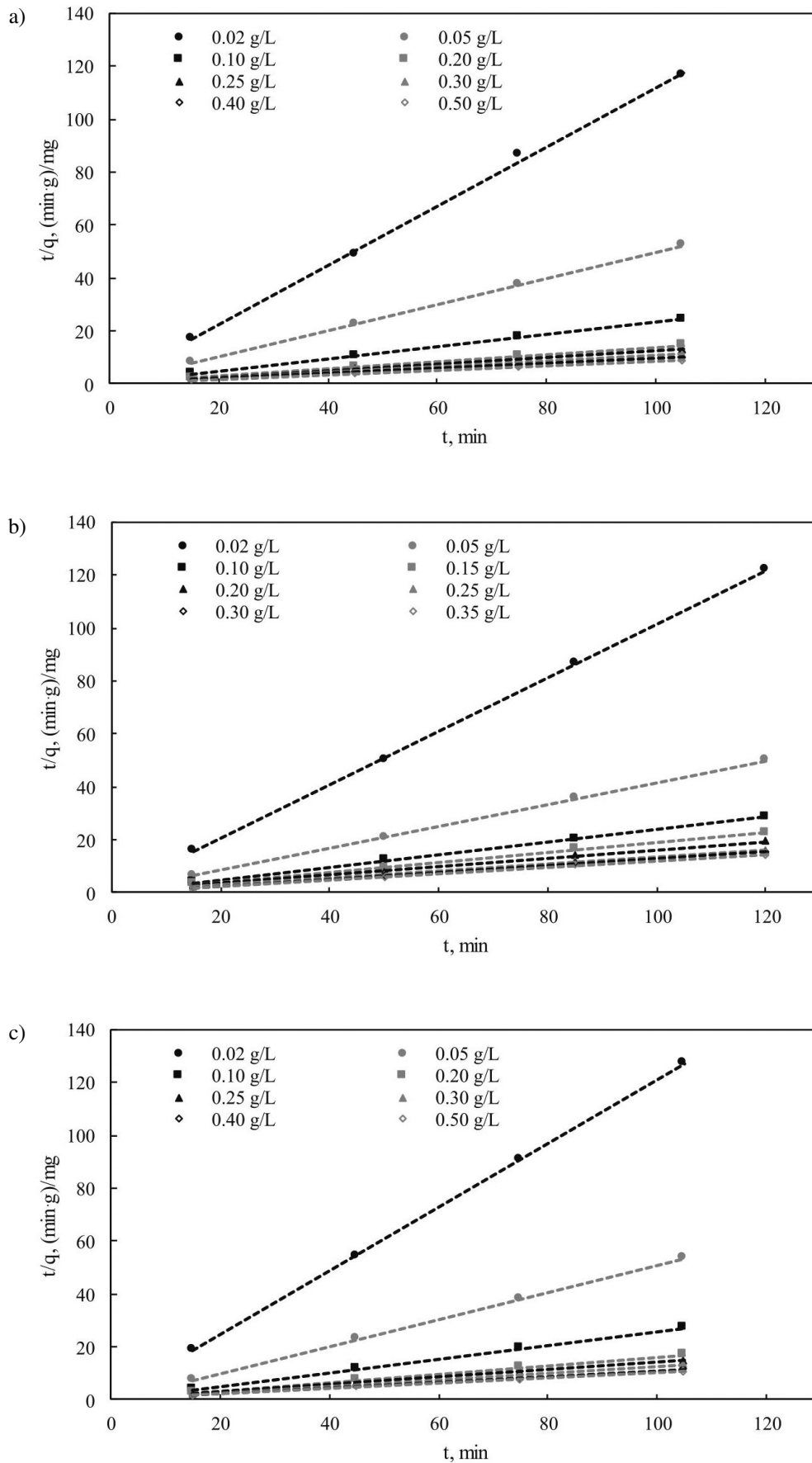*M. Borysiak, E. Gabruś, Chem. Process Eng., 2020, 41 (2), 105–117*

Fig. 3. Linear pseudo-second order kinetic model for a) pH = 3; b) pH = 7.6; c) pH = 10
and different initial concentrations of dye

Table 2. Linear pseudo-second order kinetic model constant k_2 for different pH values and initial concentrations of dye

pH = 3		pH = 7.6		pH = 10	
C_0, g/L	k_2, g/(mg·min)	C_0, g/L	k_2, g/(mg·min)	C_0, g/L	k_2, g/(mg·min)
0.02	19.382	0.02	8.992	0.02	5.744
0.20	0.095	0.15	0.166	0.20	0.113
0.25	0.082	0.20	0.081	0.25	0.081
0.30	0.054	0.25	0.084	0.30	0.128
0.40	0.073	0.30	0.267	0.40	0.094
0.50	0.037	0.35	0.047	0.50	0.041

In general, it can be stated that the pseudo-second order model describes well the kinetics of Cochineal Red A adsorption on yeast in the tested range of solution concentrations. These results indicate the crucial role of direct sorption in the rate of the whole process (Plazinski et al., 2009), but sometimes it is interpreted as the occurrence of the chemisorption mechanism (Bonilla-Petriciolet et al., 2017; Ho and McKay, 1999; Rida et al., 2013).

3.8. Intra-particle diffusion model

Pseudo-first and pseudo-second order models are not very informative in terms of exact mechanisms of mass transfer during the adsorption process. As yeast was indicated to have pores (Kim et al., 2015), intra-particle diffusion model was used to identify the mass transfer mechanism (Wang et al., 2010). The linear equation was shown below.

$$q_t = k_{dif}\sqrt{t} + C \tag{14}$$

This model may be helpful in determining the limiting mechanism in the process. Based on the shape of the model q^t vs $t^{1/2}$ plot, three possible stages (in the form of straight-lined portions of the plot) can be distinguished. The first, sharper, points to an instantaneous adsorption or external surface adsorption as the controlling mechanism. In the second segment, intra-particle diffusion begins. In the third step, the system is reaching equilibrium (Tan et al., 2007; Tan and Hameed, 2017). Intra-particle diffusion model constant C (Eq. (14)) stands for the thickness of boundary layer that may be involved in the process control (Tan and Hameed, 2017; Wang et al., 2010).

The results of linear intra-particle diffusion model fitting were shown in Fig. 4.

In the intra-particle diffusion model fittings achieved for the experimental data, either one or two stages can be distinguished. For low initial concentrations of dye (0.02–0.10 g/L), one limiting phase can be identified – the final stage where the systems approach the equilibrium. For more concentrated dye solutions (0.20–0.50 g/L) two stages of the process are visible.

These results lead to a conclusion that the limiting stage of the process is external diffusion which can be affected for example by increasing the suspension mixing intensity. The presence of pore in yeast (average pore size of 60.64 Å), reported by Kim (Kim et al., 2015), turned out to be irrelevant to mass transport and in this case, powdered yeast may be regarded as a nonporous adsorbent.
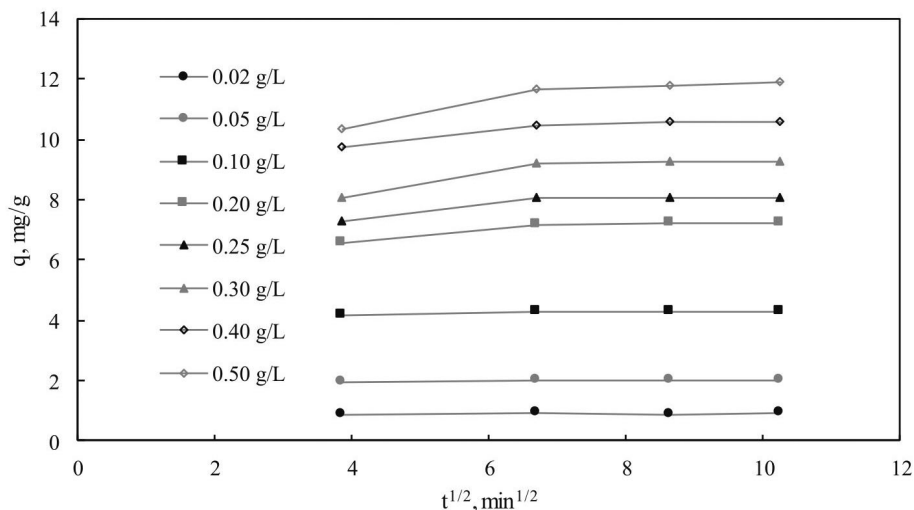
www.czasopisma.pan.pl   PAN   www.journals.pan.pl

M. Borysiak, E. Gabruś, Chem. Process Eng., 2020, 41 (2), 105–117

Fig. 4. Linear intra-particle diffusion kinetic model for pH = 3 and different initial concentrations of dye

3.9. Percentage of discoloration

The final result of adsorption process in case of dyes can be presented as the percentage of discoloration. This value, representing the amount of dye removed from the solution and expressed in percent, was calculated using Eq. (15).

$$D\% = \left(1 - \frac{C_e}{C_0}\right) \cdot 100 \tag{15}$$

The comparison of percentage of adsorption for different pH for multiple initial concentrations of dye was presented below (Fig. 5).
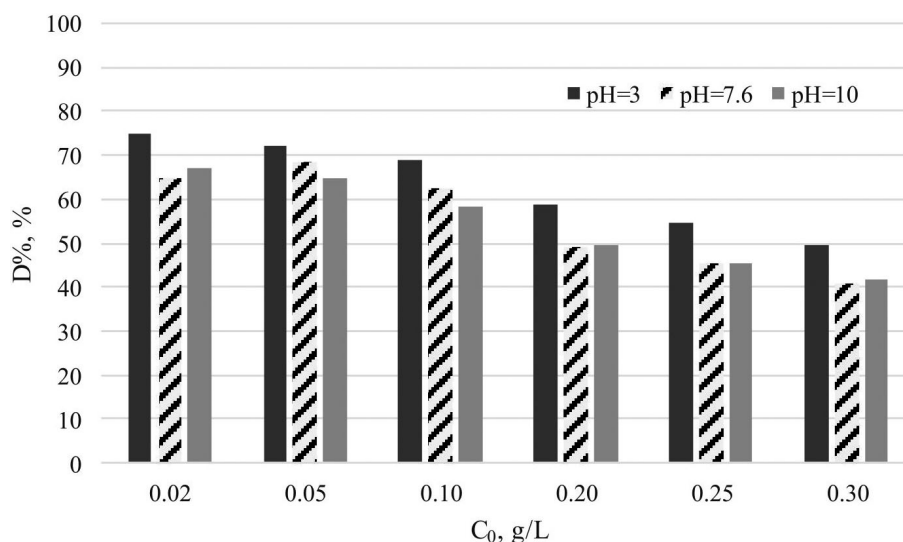

Fig. 5. Percentage of discoloration for the same initial dye concentrations and different pH values

Lower initial concentrations of the dye in the solution resulted in the increase of the discoloration effect. The addition of hydrochloric acid caused a significant rise in the dye removal process. In case of sodium hydroxide as a pH modifier, its influence on the change of the amount of the dye removed is not clear, but in terms of value considered to be insignificant.

4. CONCLUSIONS

The adsorption equilibrium in Cochineal Red A-powdered yeast aqueous system was reached after 105–120 minutes in the temperature of 30 °C. For the same initial concentration of dye, the highest achieved value of adsorption capacity was 10.16 mg/g for pH = 3. For pH = 7.6 and pH = 10 the values of adsorption capacity amounted to 8.13 and 8.38 mg/g respectively.

The adsorption equilibrium experimental results were fitted with Langmuir, Freundlich, Sips and Toth isotherm models. From four isotherm models fitted to the experimental data, Toth isotherm model demonstrated the best representation of the equilibrium for Cochineal Red A dye adsorption process on powdered yeast. The highest quality of fit of Toth isotherm model was proven by assessment with multiple methods such as coefficient of determination R^2 (values of R^2 closest to 1), average relative error δ, sum-of-squares of errors *SSE*, Chi-squared statistics χ^2, root mean sum-of-squares error *RMSE*, and normalized standard deviation Δq (lowest values of all of the error measurements in most of the cases). Langmuir and Sips isotherm models, falling slightly behind the Toth isotherm model, were also proven to have high fit quality to the experimental data. Freundlich isotherm model provided significantly lesser quality of fit to the experimental data.

The kinetics experiment results were fitted with pseudo-first order, pseudo-second order and intra-particle diffusion linearized models. Pseudo-first order model was proven to be non-representative for the experimental results. Pseudo-second order model resulted in 0.998–1.000 ranged coefficient of determination R^2, which indicates a good fit to the experimental data. Depending on the initial concentration, intra-particle diffusion model provided information about the occurrence of one (for lower initial concentrations) or two (for higher initial concentrations) stages that define the process-limiting mechanism.

The initial concentration of dye also influenced the result of the process. The lower the value of initial concentration, the more visible discoloration effect was observed. The initial concentration of dye that amounted to 0.02 g/L resulted in 64.69% (pH = 7.6) to 74.85% (pH = 3) of discoloration, while the initial concentration of 0.30 g/L resulted in 40.81% (pH = 7.6) to 49.66% (pH = 3) of discoloration.

Acidic environment provided slightly better conditions for adsorption of an azo dye, Cochineal Red A on powdered yeast. Basic environment had insignificant effect on the process in comparison to the experiment conducted with unmodified pH of the solution.

Since the results obtained are promising, further research is planned to investigate the possibilities of yeast adsorption in purifying water contaminated with other dyes. The advantages of using yeast as the adsorbent are the low cost of acquisition and no need for regeneration.

SYMBOLS

a_S	Sips isotherm model constant, $(L/g)^\beta$
a_T	Toth isotherm constant, $(g/L)^{1/T}$
b	Langmuir isotherm constant, L/g
C	intra-particle diffusion model constant, mg/g
C_0	initial concentration, g/L
C_e	equilibrium concentration, g/L
$D\%$	percentage of discoloration, %
k_1	pseudo-first order kinetic model constant, min^{-1}
k_2	pseudo-second order kinetic model constant, g/(mg·min)

www.czasopisma.pan.pl   PAN   www.journals.pan.pl

M. Borysiak, E. Gabruś, Chem. Process Eng., 2020, 41 (2), 105–117

k_{dif}	intra-particle diffusion model constant, mg/(g·s$^{1/2}$)
K_F	Freundlich isotherm constant related to adsorption capacity, (L$^{1/n}$/g$^{1/n}$)
K_S	Sips isotherm model constant, L/g
K_T	Toth isotherm constant, L/g
m_{ads}	mass of the adsorbent, g
n	adsorption intensity, –
q_{cal}	calculated equilibrium adsorption, g/g
q_e	equilibrium adsorption, g/g
q_{exp}	experimental equilibrium adsorption, g/g
$\bar{q}_{exp}$	mean experimental equilibrium adsorption, g/g
q_L	maximum adsorption capacity, g/g
q_t	adsorption at specific time, g/g
R^2	coefficient of determination, –
$RMSE$	root mean sum-of-squares error, –
SSE	sum-of-squares of errors, –
t	time, min
T	Toth isotherm constant, –
V	volume of the solution, L

Greek symbols

β	Sips isotherm model exponent, –
δ	average relative error, %
Δq	normalized standard deviation, %
χ^2	Chi-squared statistics, –

REFERENCES

Aksu Z., 2005. Application of biosorption for the removal of organic pollutants: A review. *Process Biochem.*, 40, 997–1026. DOI: 10.1016/j.procbio.2004.04.008.

Basile A., Cassano A., Rastogi N.K., 2015. *Advances in membrane technologies for water treatment – Materials, processes and applications*. Elsevier.

Bonilla-Petriciolet A., Mendoza-Castillo D.I., Reynel-Ávila H.E., 2017. *Adsorption processes for water treatment and purification*. Springer International Publishing.

El-Sayed G.O., 2011. Removal of methylene blue and crystal violet from aqueous solutions by palm kernel fiber. *Desalination*, 272, 225–32. DOI: 10.1016/j.desal.2011.01.025.

Foo K.Y., Hameed B.H., 2010. Insights into the modeling of adsorption isotherm systems. *Chem. Eng. J.*, 156, 2–10. DOI: 10.1016/j.cej.2009.09.013.

Frantz T.S., Silveira N., Quadro M.S., Andreazza R., Barcelos A.A., Cadaval T.R.S. Jr., Pinto L.A.A., 2017. Cu(II) adsorption from copper mine water by chitosan films and the matrix effects. *Environ. Sci. Pollut. Res.*, 24, 5908–5917. DOI: 10.1007/s11356-016-8344-z.

Gerente C., Lee V.K.C., Le Cloirec P., McKay G., 2007. Application of chitosan for the removal of metals from wastewaters by adsorption—mechanisms and models review. *Crit. Rev. Environ. Sci. Technol.*, 37, 41–127. DOI: 10.1080/10643380600729089.

Gupta V.K., Suhas, 2009. Application of low-cost adsorbents for dye removal – A review. *J. Environ. Manage*, 90, 2313–2342. DOI: 10.1016/j.jenvman.2008.11.017.

Heibati B., Rodriguez-Couto S., Al-Ghouti M.A., Asif M., Tyagi I., Agarwal S., Gupta V.K., 2015. Kinetics and thermodynamics of enhanced adsorption of the dye AR 18 using activated carbons prepared from walnut and poplar woods. *J. Mol. Liq.*, 208, 99–105. DOI: 10.1016/j.molliq.2015.03.057.

Ho Y.S., McKay G., 1999. Pseudo-second order model for sorption processes. *Process Biochem.*, 34, 451–465. DOI: 10.1016/S0032-9592(98)00112-5.

Ho Y.S., Porter J.F., McKay G., 2002. Equilibrium isotherm studies for the sorption of divalent metal ions onto peat: copper, nickel and lead single component systems. *Water Air Soil Pollut.*, 141, 1–33. DOI: 10.1023/A:1021304828010.

Howe K.J., Hand D.W., Crittenden J.C., Trussell R.R., Tchobanoglous G., 2012. *Principles of Water Treatment*. John Wiley & Sons.

Kavitha D., Namasivayam C., 2007. Experimental and kinetic studies on methylene blue adsorption by coir pith carbon. *Bioresour. Technol.*, 98, 14–21. DOI: 10.1016/j.biortech.2005.12.008.

Kim T.-Y., Lee J.-W., Cho S.-Y., 2015. Application of residual brewery yeast for adsorption removal of Reactive Orange 16 from aqueous solution. *Adv. Powder Technol.*, 26, 267–274. DOI: 10.1016/j.apt.2014.10.006.

Montgomery D.C., Peck E.A., Vining G.G., 2012. *Introduction to Linear Regression Analysis*. *Wiley*.

Plazinski W., Rudzinski W., Plazinska A., 2009. Theoretical models of sorption kinetics including a surface reaction mechanism: A review. *Adv. Colloid Interface Sci.*, 152, 2–13. DOI: 10.1016/j.cis.2009.07.009.

Rafatullah M., Sulaiman O., Hashim R., Ahmad A. (2010). Adsorption of methylene blue on low-cost adsorbents: A review. *J. Hazard. Mater.*, 177, 70–80. DOI: 10.1016/j.jhazmat.2009.12.047.

Rehman S., Adil A., Shaikh A.J., Shah J.A., Arshad M., Ali M.A., Bilal M., 2018. Role of sorption energy and chemisorption in batch methylene blue and Cu^{2+} adsorption by novel thuja cone carbon in binary component system: linear and nonlinear modeling. *Environ. Sci. Pollut. Res.*, 25, 31579–31592. DOI: 10.1007/s11356-018-2958-2.

Rida K., Bouraoui S., Hadnine S., 2013. Adsorption of methylene blue from aqueous solution by kaolin and zeolite. *Appl. Clay Sci.*, 83–84, 99–105. DOI: 10.1016/j.clay.2013.08.015.

Shokoohi R., Vatanpoor V., Zarrabi M., Vatani A., 2010. Adsorption of Acid Red 18 (AR18) by activated carbon from poplar wood - A kinetic and equilibrium study. *E-J. Chem.*, 7. DOI: 10.1155/2010/958073.

Tan I.A.W., Hameed B.H., Ahmad A.L., 2007. Equilibrium and kinetic studies on basic dye adsorption by oil palm fibre activated carbon. *Chem. Eng. J.*, 127, 111–9. DOI: 10.1016/j.cej.2006.09.010.

Tan K.L., Hameed B.H., 2017. Insight into the adsorption kinetics models for the removal of contaminants from aqueous solutions. *J. Taiwan Inst. Chem. Eng.*, 74, 25–48. DOI: 10.1016/j.jtice.2017.01.024.

Vijayaraghavan K., Padmesh T.V.N., Palanivelu K., Velan M., 2006. Biosorption of nickel(II) ions onto *Sargassum wightii*: Application of two-parameter and three-parameter isotherm models. *J. Hazard. Mater.*, 133, 304–308. DOI: 10.1016/j.jhazmat.2005.10.016.

Wang L., Zhang J., Zhao R., Li C., Li Y., Zhang C., 2010. Adsorption of basic dyes on activated carbon prepared from *Polygonum orientale* Linn: Equilibrium, kinetic and thermodynamic studies. *Desalination*, 254, 68–74. DOI: 10.1016/j.desal.2009.12.012.

Worch E., 2012. *Adsorption technology in water treatment - Fundamentals, processes, and modeling*. De Gruyter.

Yagub M.T., Sen T.K., Afroze S., Ang H.M., 2014. Dye and its removal from aqueous solution by adsorption: A review. *Adv. Colloid Interface Sci.*, 209, 172–184. DOI: 10.1016/j.cis.2014.04.002.

Yuh-Shan H., 2004. Citation review of Lagergren kinetic rate equation on adsorption reactions. *Scientometrics*, 59, 171–177. DOI: 10.1023/B:SCIE.0000013305.99473.cf.